

Amplification of waves by submerged plates

J. N. Newman
jnn@mit.edu

(Submitted to the 30th IWWFEB – Bristol, UK – 12-15 April 2015)

1 Introduction

The possibility of using submerged structures to focus waves is of special interest for wave-energy converters. Mehlum and Stamnes used a ‘wave lens’ in a large outdoor experimental facility (cf. [1] and references therein). Subsequent analyses have been made by Murashige & Kinoshita [2], Teigen [3], Griffiths & Porter [4], and others. Most of this work is motivated by the concept of optical refraction, at least as a first approximation, which implies that the structure is large relative to the wavelength λ . The lens described in [1] is a transverse array of small elements extending over a width of 33λ , with amplification factors of 3-4 at the focal point. Slender-body approximations are used in [2] to achieve amplification factors of 5 with a width of 16λ . Submerged plates with simple planforms and smaller dimensions are used in [3], with amplification factors of 2. Bathymetry with an elliptical plateau is considered in [4], with horizontal dimensions on the order of 10λ and amplification factors of 4-4.5. (The amplification factor is defined here as the maximum value of the free-surface elevation, for an incident wave of unit amplitude.) For the configurations in [3] and [4] the point of maximum elevation is in the shallow region above the plate or plateau.

For practical applications it is desirable to reduce the size of the structure. In the present work submerged horizontal plates are considered with dimensions comparable to the wavelength. Instead of assuming a simple geometrical shape, the planform is represented by a Fourier series with optimized coefficients to maximize the amplification factor. The computational approach combines the multi-variate optimization code PRAXIS with the radiation/diffraction code WAMIT, as in [5]. Planforms are found with amplification factors between 5 and 15 at one wavenumber. Other planforms are found which maximize the average amplitude over a range of wavenumbers. As in [3] and [4] the point of maximum amplitude is in the shallow region above the plate. This may be an important restriction for wave-energy converters, since the power may be substantially less than for a plane progressive wave with the same amplitude.

2 Formulation

Plane waves of unit amplitude and wavenumber K propagate in the $+x$ -direction toward a submerged horizontal plate of zero thickness. The fluid depth is infinite and linear potential theory is assumed. The plate is stationary, and occupies the space $0 \leq r \leq R(\theta)$ in the plane $z = -d$, where d is the depth below the undisturbed free surface and (r, θ) are polar coordinates with $x = r \cos \theta$, $y = r \sin \theta$. The coordinates and wavenumber are nondimensional. Symmetry is assumed about $y = 0$, and the outer radius R is represented by the Fourier series

$$R(\theta) = \sum_{n=0}^N c_n \cos n\theta. \quad (1)$$

The free surface is defined as $z = \text{Re} [\zeta(x, y)e^{i\omega t}]$, where ω is the wave frequency and $K = \omega^2/g$. The amplification factor A is defined as the maximum value of $|\zeta(x, y)|$ over the domain of the free surface. The coefficients c_n are determined by optimization, with the objective to maximize A . The ‘half-length’ $a = R(0)$ is fixed to constrain the size of the plate, with the value $a = 2$. Except where noted the wavenumber $K = 1$ is used for the optimizations.

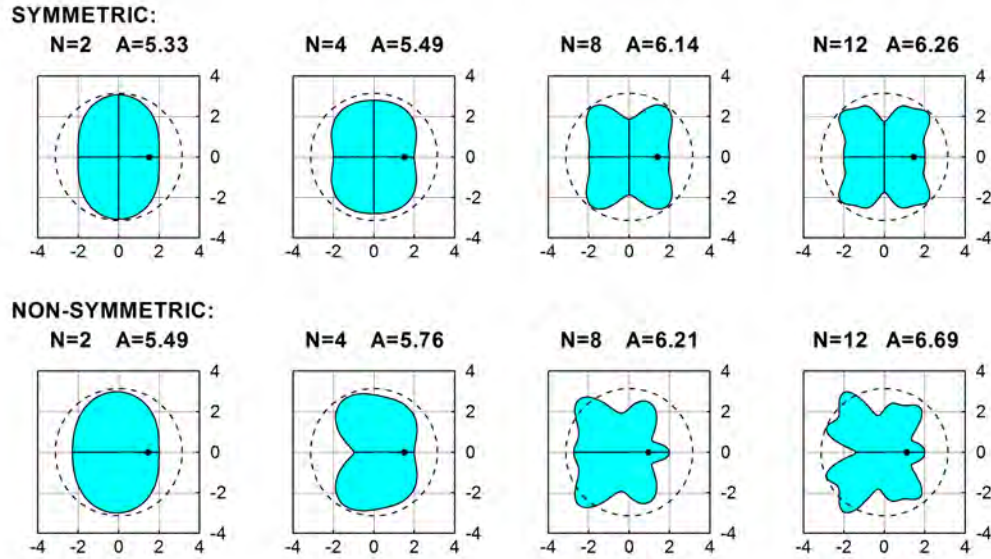


Figure 1: Planforms of the plates defined by the Fourier series (1) with $N = 2, 4, 8, 12$ and $d = 0.25$. The diameter of the dashed circles is equal to the wavelength 2π of the incident waves, which propagate from left to right. The maximum amplitude A occurs at the points shown by filled black circles.

3 Results

Figure 1 shows the planforms of optimized plates for the depth $d = 0.25$, with the upper limit N of the Fourier series equal to 2,4,8,12. Only the Fourier coefficients of even order are used in the upper row, to represent plates which are symmetrical about $x = 0$. In the lower row all $N + 1$ coefficients are included to allow for non-symmetry. The parameter A increases with increasing N , but at a relatively slow rate. Allowing for non-symmetry introduces interesting details in the planform, but does not increase the maximum amplitude substantially.

The diameter of the dashed circles in Figure 1 is equal to the wavelength of the incident waves in deep water. Accounting for the finite depth above the plates reduces the wavelength by about one half. Thus the planforms in Figure 1 have maximum dimensions which are approximately equal to one deep-water wavelength, or two wavelengths for waves of the same frequency in depth d .

Figure 2 shows the planforms of symmetrical plates with $N = 8$, for different values of the depth d . The Fourier coefficients for these plates are listed in Table 1. The planform with $d = 0.25$ differs from the corresponding plate in Figure 1, due to the different initial conditions used for each optimization. This is an example of local convergence of the optimizations, which are not unique, and other planforms may exist with larger values of A . (Another planform was found for $d = 0.15$ with $A = 19.02$, but with twice the width of the plate shown here.)

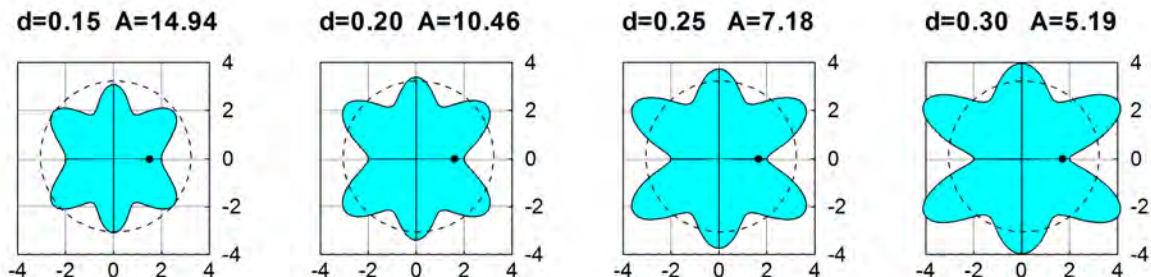


Figure 2: Planforms of symmetrical plates defined by the Fourier series (1) with $N = 8$ and depths d as shown.

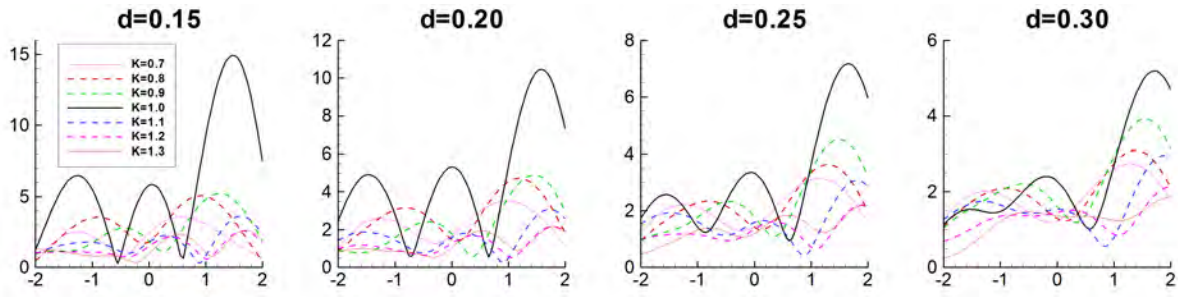


Figure 3: Free-surface elevation $|\zeta|$ as a function of the position x along the centerline of the plates shown in Figure 2, for different values of the wavenumber K . Note that the vertical scales are different.

The free-surface elevations $|\zeta(x, 0)|$ above the plates in Figure 2 are plotted in Figure 3, for different values of the wavenumber K . The solid curves correspond to the wavenumber $K = 1$ used for the optimizations. For other values of K the amplification factors are reduced substantially.

Figure 4 shows planforms which are optimized for a range of wavenumbers. Here the average of the amplitudes at seven uniformly-spaced wavenumbers $K = 0.7(0.1)1.3$ is used, instead of the amplitude at $K = 1$, and \bar{A} is defined as the maximum value of this average at all the field points x . The Fourier coefficients are listed in Table 2. The corresponding elevations of the free surface are shown in Figure 5. In these cases the maximum amplitudes occur at longer wavelengths ($K < 1$). These planforms are smaller and the free-surface elevations are more uniform with respect to the wavenumber K , but the maximum amplitudes are much less than for the plates in Figure 2.

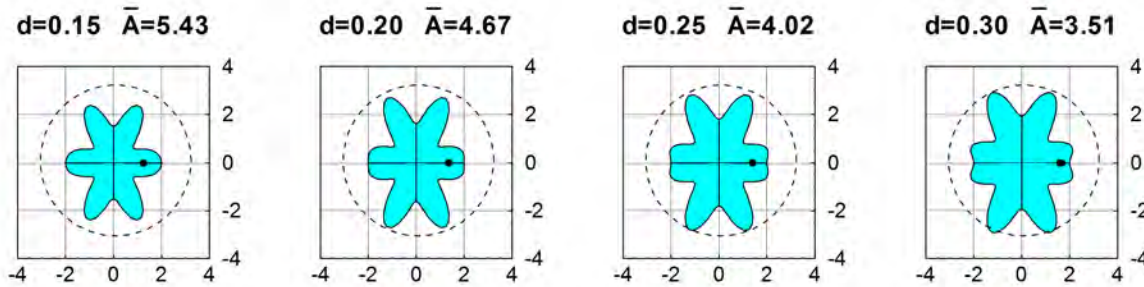


Figure 4: Planforms of the symmetric plates optimized for the range of wavenumbers $0.7 \leq K \leq 1.3$. The diameter of the dashed circles is equal to the wavelength at $K = 1$.

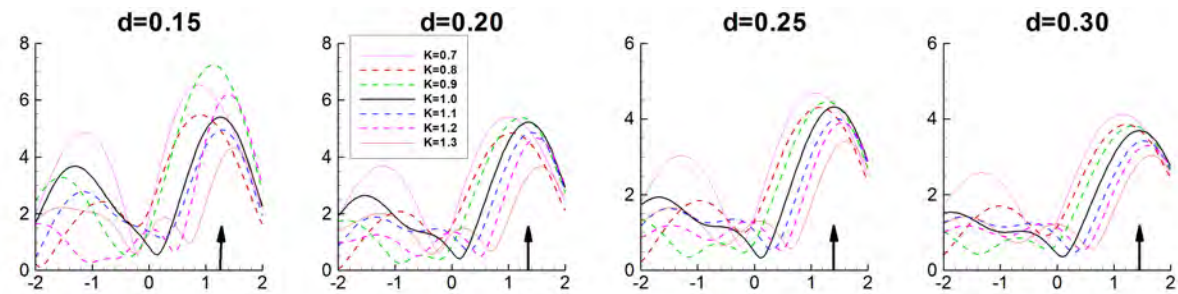


Figure 5: Free-surface elevation $|\zeta|$ as a function of the position x along the centerline of the plates shown in Figure 4, for different values of the wavenumber K . The vertical arrows show the points x where the averaged amplitude has its maximum value \bar{A} .

4 Conclusions

Submerged horizontal plates are found with planforms which maximize the local amplitude of the free-surface elevation. These plates are relatively compact, with horizontal dimensions comparable to the wavelength. Amplification factors between 5 and 15 are achieved at the wavenumber $K = 1$ used for the optimizations, but these factors are reduced substantially at other wavenumbers. An alternative set of plates are optimized for the range of wavenumbers $0.7 \leq K \leq 1.3$, with their average amplitude factors \bar{A} between 3.5 and 5.4. Some reduction of the amplitude is expected for oblique waves, but this may be less important in a typical spectrum compared to the effect of different frequencies and corresponding wavenumbers.

For applications to wave-energy converters it should be noted that the point of maximum amplification is above the plate, where the elevation of the free surface is affected by three-dimensional effects and by reflection at the edge of the plate. Thus the relation between the amplitude of free-surface elevation and the power is more complicated than for a plane progressive wave and the available power may be much less than would be implied by a simple analysis based on the maximum amplitude. An interesting possible extension of the present work would be to combine a simple point absorber with a submerged plate and optimize both to maximize the power output.

Viscous and nonlinear effects are obvious issues. Separation may be mitigated by using finite thickness with a rounded edge. Nonlinear effects are important if the amplitude is comparable to the depth of the plate. Notwithstanding these practical issues, it is surprising that such large amplification factors can be achieved simply by optimizing the planform, when the dimensions are comparable to the wavelength.

References

- [1] Stannnes, J.J., Løvhaugen, O., Spjelkavik, B., Mei, C.C., Lo, E. & Yue, D.K.P. ‘Nonlinear focusing of surface waves by a lens - theory and experiment,’ *J. Fluid Mech.* **135**, 71-94 (1983).
- [2] Murashige, S. & Kinoshita, T. ‘An ideal ocean wave focusing lens and its shape,’ *Applied Ocean Research* **14**, 275-290 (1992).
- [3] Teigen, P. ‘On wave amplification over submerged lenses,’ 23rd IWWFEB, Jeju, Korea (2008).
- [4] Griffiths, L.S. & Porter, R. ‘Focusing of surface waves by variable bathymetry,’ *Applied Ocean Research* **34**, 150-163 (2012).
- [5] Newman, J.N. ‘Cloaking a circular cylinder in deep water,’ 28th IWWFEB, l’Isle sur la Sorgue, France (2013).

| d | A | c_0 | c_2 | c_4 | c_6 | c_8 |
|------|-------|--------|---------|---------|---------|---------|
| 0.15 | 14.94 | 2.5609 | -0.0570 | -0.2119 | -0.4854 | 0.1934 |
| 0.20 | 10.46 | 2.9254 | -0.1069 | -0.3614 | -0.5967 | 0.1397 |
| 0.25 | 7.18 | 3.2355 | -0.0508 | -0.3449 | -0.8274 | -0.0123 |
| 0.30 | 5.19 | 3.4775 | -0.0179 | -0.3254 | -0.9663 | -0.1679 |

Table 1: Fourier coefficients of the plates shown in Figure 2.

| d | \bar{A} | c_0 | c_2 | c_4 | c_6 | c_8 |
|------|-----------|--------|---------|--------|--------|---------|
| 0.15 | 5.43 | 1.7807 | -0.2641 | 0.2219 | 0.5128 | -0.2514 |
| 0.20 | 4.67 | 1.9693 | -0.3242 | 0.2058 | 0.5221 | -0.3730 |
| 0.25 | 4.02 | 2.0953 | -0.3441 | 0.1998 | 0.4515 | -0.4025 |
| 0.30 | 3.51 | 2.2020 | -0.3514 | 0.1833 | 0.3869 | -0.4207 |

Table 2: Fourier coefficients of the plates shown in Figure 4.